LARGE EDDY SIMULATION OF HEAVY TURBULENT THERMAL

Xinya YING[1], Juichiro AKIYAMA[2], Masaru URA[3], Yayoi NAKANISHI[1]

[1] Student Member of JSCE, Graduate Student, Graduate School of Engineering, Kyushu Institute of Technology (1-1 Sensuicho, Tobataku, Kitakyushu 804-8550, Japan)
[2] Member of JSCE, Associated Professor, Dept. of Civil Engineering, Kyushu Institute of Technology
[3] Member of JSCE, Professor, Dept. of Civil Engineering, Kyushu Institute of Technology

The motion of a 2-D heavy turbulent thermal is studied by large eddy simulations. The governing equations consist of the filtered 2-D Navier-Stokes equations and mass conservation equation and are solved using the combined cubic spline (CCS) scheme. The eddy viscosity is evaluated by the Smagorinsky model.

The comparisons of computational results of main flow characteristics, including shape, size, mass center velocity and average buoyant force, with experimental results show that the numerical model gives a good description of the thermal. It is also demonstrated from the computation that the internal flow of the thermal is characterized by two symmetrical vortex structures and the density excess becomes a double-peak distribution after some distance.

Key Words *: Thermals, density current, LES, Smagorinsky model, CCS scheme*

1. INTRODUCTION

A heavy turbulent thermal is defined as an instantaneous release of dense fluid into a less dense ambient fluid (see Fig. 1). The dense fluid will freely fall and spread under the influence of its own buoyant force. A practical example of the thermal is dumping sludge or soil into coastal waters using bottom-dump barges, which is often encountered in construction of man-made islands etc. If the density of the fluid is less than that of the ambient, it is referred to as a light turbulent thermal. The upward motion of the hot cloud formed by explosion is an example of a light turbulent thermal. Essentially, both heavy and light thermals have the same internal flow structure, so that they are usually referred to as turbulent thermals.

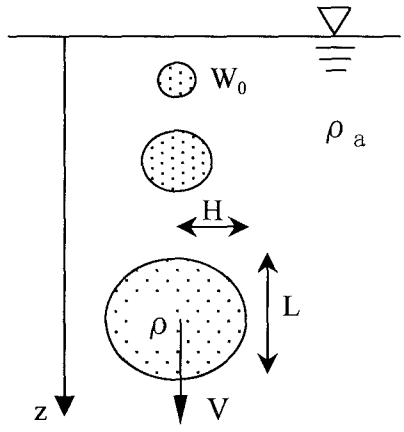

Fig.1 Definition sketch of heavy turbulent thermal

To understand the flow characteristics of the thermal, a great deal of study has been performed. In 1957, Scorer[1)] obtained empirical equations on the width and the front position of the thermal. Wang[2)] developed a model for the motion of a turbulent buoyant thermal in a calm, stably stratified atmosphere, based on the conservation of mass, vertical momentum and enthalpy. Using this model, the average motion of the thermal is described in terms of its initial density difference, velocity and effective radius as well as mass entrainment constant, effective drag coefficient and turbulent dissipation rate. But, the added mass is ignored in this model. In addition, the model was not verified by experimental data. Escudier and Maxworthy[3)] proposed a model to describe the average motion of the thermal based on the conservation of momentum and mass. In this model, the added mass is included. But the drag force acted on the thermal body is ignored. Again, this model was not verified by

experimental data. Baines and Hopfinger[4] experimentally and theoretically investigated the thermal with large density difference and indicated that the effects of large density difference are confined to the region close to the source. Akiyama et al.[5] conducted a series of experiment on 2-D heavy turbulent thermals and developed an integral model to predict such flow characteristics as half width, velocity and average buoyant force. In this model, both added mass and drag force are included. The entrainment coefficient and the drag coefficient are determined based on a large number of experimental data. Nakatsuji et al.[6] made an experimental study on particle thermals, which are formed by an instantaneous release of a cloud of particles into water, and found that the average motion of the particle thermal is close to that of the thermal formed by dense fluid if the initial volume of cloud is relatively large and the size of particles is relatively small.

The aforementioned thermal models are essentially based on similarity in thermal shape. Such analyses are useful to understand the fundamentals of the motion of the thermal in a fully developed state. However, heavy turbulent thermals in practice take place in complicated conditions, such as the presence of a density gradient, the occurrence of a current, the limitation of ambient water depth and others. It necessitates development of a numerical model. Li[7] studied particle thermals experimentally and numerically employing a mixing length model, and found that the velocity of the thermal approaches the terminal velocity of the individual particles and the growth rate of half width of thermal decreases with the magnitude of the settling velocity of particles. Tamai and Muraoka[8] investigated turbidity transport produced by direct dumping of soil using the two-fluid k- ε turbulence model and found that the induced flow is depressed by slowing down the dump of soil.

In the present work, an attempt is made to develop a numerical model for a 2-D heavy turbulent thermal by using the large eddy simulation (LES) with the Smagorinsky model.

2. MODEL FORMULATION

Applying the grid filter to the 2-D incompressible Navier-Stokes equations and the equation of conservation of mass, we can obtain the governing equations

$$\frac{\partial U_i}{\partial x_i} = 0 \tag{1}$$

$$\frac{\partial U_i}{\partial t} + U_j \frac{\partial U_i}{\partial x_j} = -\frac{1}{\rho}\frac{\partial P}{\partial x_i} + \nu \frac{\partial^2 U_i}{\partial x_j^2} + \frac{\partial}{\partial x_j}\left(-\overline{u_i' u_j'}\right) + g_i \frac{\Delta \rho}{\rho} \tag{2}$$

$$\frac{\partial \Delta \rho}{\partial t} + U_i \frac{\partial \Delta \rho}{\partial x_i} = \frac{\partial}{\partial x_i}\left(-\overline{u_i' \Delta \rho'}\right) \tag{3}$$

where U_i is the large-scale quantities of velocity component in the direction x_i; P the large-scale pressure minus the hydrostatic pressure at reference density ρ_a; ρ the large-scale density; $\Delta \rho$ the density excess ($= \rho - \rho_a$); g_i the specific body force in the direction x_i; $u_i', \Delta\rho'$ the fluctuating velocity and density excess. $\overline{u_i' u_j'}$ the correlation terms between fluctuating velocity due to space averaging. By using eddy viscosity concept, the correlation terms take the form

$$-\overline{u_i' u_j'} = \nu_t\left(\frac{\partial U_i}{\partial x_j} + \frac{\partial U_j}{\partial x_i}\right) - \frac{2}{3} k \delta_{ij} \tag{4}$$

where ν_t is the subgrid scale eddy viscosity; k the turbulent kinetic energy ; δ_{ij} the Kronecker delta function. The last term in Eq. (4) represents the normal stresses and can be absorbed in the pressure terms of the momentum equations.

In the Smagorinsky model, ν_t is calculated by

$$\nu_t = (Cs\,\Delta)^2 |\bar{S}| \tag{5}$$

where Δ is the filter width, Cs is the Smagorinsky constant, and $|\bar{S}| = (2\bar{S}_{ij}\bar{S}_{ij})^{1/2}$ is the magnitude of large-scale strain rate tensor in which $\bar{S}_{ij}$ is defined by

$$\bar{S}_{ij} = \frac{1}{2}\left(\frac{\partial U_i}{\partial x_j} + \frac{\partial U_j}{\partial x_i}\right) \tag{6}$$

The term $-\overline{u_i' \Delta \rho'}$ in Eq. (3) is generally assumed to be

$$-\overline{u_i' \Delta \rho'} = \frac{\nu_t}{Scs}\frac{\partial \Delta \rho}{\partial x_i} \tag{7}$$

where Scs is the subgrid turbulent Schmidt number and is defined as the ratio of eddy diffusivity of momentum to eddy diffusivity of matter.

Using the operator-split algorithm, the governing equations for flow, namely, Eqs. (1) and (2) are divided into the following two steps:

1) Advection and Diffusion

$$\frac{\partial U_i}{\partial t} + U_j \frac{\partial U_i}{\partial x_j} = \nu \frac{\partial^2 U_i}{\partial x_j^2} + \frac{\partial}{\partial x_j}\left(\nu_t \left(\frac{\partial U_i}{\partial x_j} + \frac{\partial U_j}{\partial x_i} \right) \right)$$

$$[n\Delta t \le t \le (n+\frac{1}{2})\Delta t] \tag{8}$$

2) Pressure

$$\frac{\partial U_i}{\partial x_i} = 0 \tag{9}$$

$$\frac{\partial U_i}{\partial t} = -\frac{1}{\rho}\frac{\partial P}{\partial x_i} + g_i \frac{\Delta \rho}{\rho} \tag{10}$$

$$[(n+\frac{1}{2})\Delta t \le t \le (n+1)\Delta t]$$

The density excess and velocity are obtained by solving Eqs. (3) and (8) using the combined cubic spline (CCS) scheme described below. The pressure is obtained by solving the Poisson type equation deduced from the algebraic manipulation of Eqs.(9) and (10).

The CCS scheme for 2-D advection and diffusion problems is as follows. The 2-D advection and diffusion equation can be expressed in the form

$$\frac{\partial f}{\partial t} + u\frac{\partial f}{\partial x} + v\frac{\partial f}{\partial y} = D\frac{\partial^2 f}{\partial x^2} + D\frac{\partial^2 f}{\partial y^2} \tag{11}$$

where f is a scalar, u and v are velocity component in x and y direction, and D is a diffusion coefficient. If the time derivatives are expressed by a combined algorithm, and the spatial distribution of scalar f is fitted by a series of cubic spline passing through grid points $\{x_1, y_j\}, \{x_2, y_j\}, \ldots, \{x_I, y_j\}$, j=1, 2,$\cdots$, J for x-direction and $\{x_i, y_1\}, \{x_i, y_2\}, \ldots, \{x_i, y_J\}$, i=1, 2,$\cdots$, I for y-direction (see Fig.2), Eq. (11) is transformed to

$$\frac{f_{i,j}^{n+1} - f_{i,j}^{n}}{\Delta t} = \theta\,(D_{i,j}^{n} Mx_{i,j}^{n} + D_{i,j}^{n} My_{i,j}^{n} - u_{i,j}^{n} Nx_{i,j}^{n} - v_{i,j}^{n} Ny_{i,j}^{n}) + (1-\theta)(D_{i,j}^{n+1} Mx_{i,j}^{n+1} + D_{i,j}^{n+1} My_{i,j}^{n+1} - u_{i,j}^{n+1} Nx_{i,j}^{n+1} - v_{i,j}^{n+1} Ny_{i,j}^{n+1}) \tag{12}$$

in which

$$Nx_{i,j}^{n} = \left.\frac{\partial f}{\partial x}\right|_{i,j}^{n} \qquad Mx_{i,j}^{n} = \left.\frac{\partial^2 f}{\partial x^2}\right|_{i,j}^{n}$$

$$Ny_{i,j}^{n} = \left.\frac{\partial f}{\partial y}\right|_{i,j}^{n} \qquad My_{i,j}^{n} = \left.\frac{\partial^2 f}{\partial y^2}\right|_{i,j}^{n}$$

θ is a weight coefficient ($0 \le \theta \le 1$), for explicit scheme θ =1, for fully implicit scheme θ =0, for the scheme similar to Crank-Nicolson θ =0.5. For the cubic spline interpolation passing through the grid points $\{x_1, y_j\}, \{x_2, y_j\}, \ldots\ldots, \{x_I, y_j\}$, we can obtain[9]

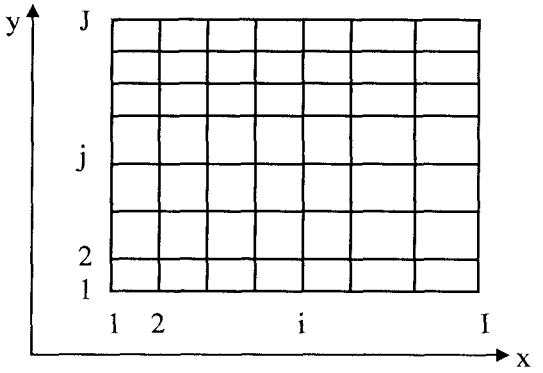

Fig.2 Sketch of mesh for 2-D CCS scheme

$$\frac{\Delta x_{i-1}}{6} Mx_{i-1,j}^{n} + \frac{\Delta x_{i-1} + \Delta x_i}{3} Mx_{i,j}^{n} + \frac{\Delta x_i}{6} Mx_{i+1,j}^{n} = \frac{f_{i+1,j}^{n} - f_{i,j}^{n}}{\Delta x_i} - \frac{f_{i,j}^{n} - f_{i-1,j}^{n}}{\Delta x_{i-1}} \quad (i = 2, I-1) \tag{13}$$

in which $\Delta x_i = x_{i+1} - x_i$.

$Mx_{1,j}^{n}$ and $Mx_{i,j}^{n}$ are determined according to the boundary conditions. Then, $Mx_{i,j}^{n}(i = 2, I-1)$ can be determined by Eq. (13). $Nx_{i,j}^{n}(i = 1, I)$ is calculated by the equations

$$Nx_{1,j}^{n} = -\left(\frac{Mx_{1,j}^{n}}{3} + \frac{Mx_{2,j}^{n}}{6}\right)\Delta x_1 + \frac{f_{2,j}^{n} - f_{1,j}^{n}}{\Delta x_1} \tag{14}$$

$$Nx_{i,j}^{n} = \left(\frac{Mx_{i,j}^{n}}{3} + \frac{Mx_{i-1,j}^{n}}{6}\right)\Delta x_{i-1} + \frac{f_{i,j}^{n} - f_{i-1,j}^{n}}{\Delta x_{i-1}} \quad (i = 2, I) \tag{15}$$

Similarly, for the cubic spline interpolation passing through the grid points $\{x_i, y_1\}, \{x_i, y_2\}, \ldots\ldots, \{x_i, y_J\}$, we can obtain

$$\frac{\Delta y_{j-1}}{6} My_{i,j-1}^{n} + \frac{\Delta y_{j-1} + \Delta y_j}{3} My_{i,j}^{n} + \frac{\Delta y_j}{6} My_{i,j+1}^{n} = \frac{f_{i,j+1}^{n} - f_{i,j}^{n}}{\Delta y_j} - \frac{f_{i,j}^{n} - f_{i,j-1}^{n}}{\Delta y_{j-1}} \quad (j = 2, J-1) \tag{16}$$

in which $\Delta y_j = y_{j+1} - y_j$.

$My_{i,1}^{n}$ and $My_{i,J}^{n}$ are determined according to the boundary conditions. Then, $My_{i,j}^{n}(i = 2, I-1)$ can be determined by Eq. (16). $Ny_{i,j}^{n}(j = 1, J)$ is calculated by the equations

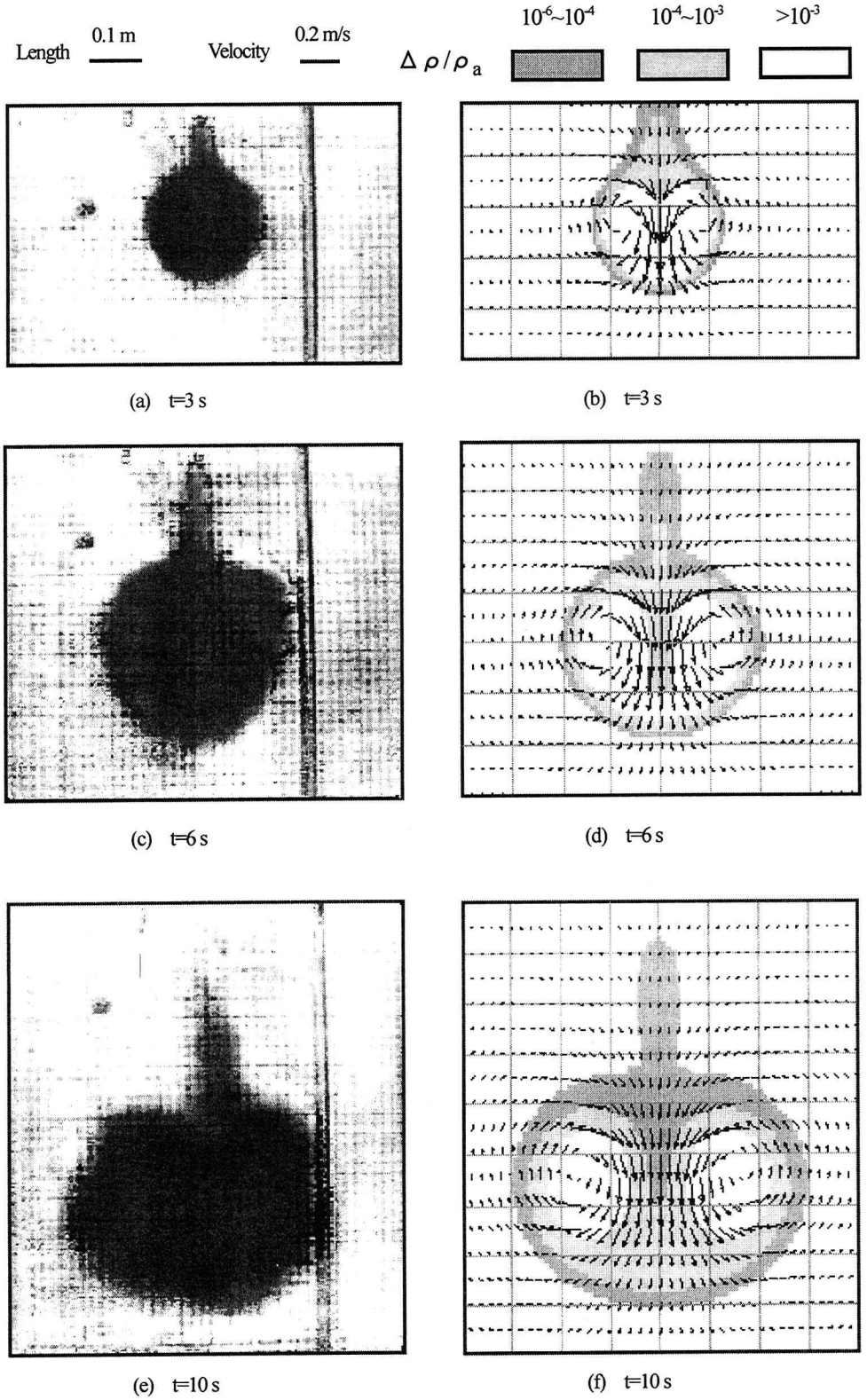

Fig.3 Photographs and computed velocity and density excess fields
(a),(c) and (e) are photographs; (b),(d) and (f) are computational results

$$Ny^n_{i,1} = -\left(\frac{My^n_{i,1}}{3} + \frac{My^n_{i,2}}{6}\right)\Delta y_1 + \frac{f^n_{i,2} - f^n_{i,1}}{\Delta y_1} \quad (17)$$

$$Ny^n_{i,J} = \left(\frac{My^n_{i,J}}{3} + \frac{My^n_{i,J-1}}{6}\right)\Delta y_{J-1} + \frac{f^n_{i,J} - f^n_{i,J-1}}{\Delta y_{j-1}} \quad (j=2,J) \quad (18)$$

Finally, $f^{n+1}_{i,J}$ (i=1,2,$\cdots$,I and j=1,2,$\cdots$,J) are obtained by solving Eq.(12). If θ is not equal to 1, iteration technique is employed in solving Eq.(12). The CCS scheme has been found to be advantageous in solving the advection and diffusion equation because its remarkable accuracy and simplicity as well as the ability to be easily extended to multi-dimensional problems[10].

3. THE EXPERIMENTAL AND COMPUTATIONAL CONDITIONS

In order to verify the numerical model, experiments on 2-D heavy turbulent thermals were performed in a glass flume of 7.5m length, 1.0m height and 0.1m width. Salt solution was used to produce the thermals. The initial total buoyant force W_0 was fixed at 0.001764 m^3/s^2. W_0 is defined as $W_0 = A_0 g(\rho_0 - \rho_a)/\rho_a$, where ρ_0 and A_0 are density and cross-section area of the source, g is the gravity acceleration. The dense fluid was released into acquiescent water by a device which is placed just above the water surface. The motion of thermal was recorded by a video camera and the pictures were analyzed to obtain such flow characteristics as shape, size (H, L), mass center velocity V and average density B. The experiment was repeated five times under the same conditions to reduce uncertainty.

The computational domain is a rectangle of 2.0m width and 1.4m height. All boundaries are considered as a slip wall boundary. The source of the thermal is a circle with a radius of 0.04m and is centered at the water depth = 0.1m. The thermal is assumed to start from rest. The total buoyant force has the same value as that in the experiment. The density of ambient fluid is 1000 kg/m^3. Grid size is 0.01 m$\times$0.01 m. The time step size is 0.025 s. The values of Cs and Scs are Cs=0.16 and Scs=0.1, according to the study on inclined plumes[11].

4. RESULTS

Fig.3 shows experimental photographs of the thermal as well as computed velocity and density excess fields at time t=3, 6 and 10 s. It is seen from this figure that shape, size and mass center velocity of the thermal obtained by computation agree well with that by experiment, although the shape of the thermal in experiment is slightly irregular because of the unsteady nature of the flow. The wake of thermal appears in both computational and experimental results. However, the buoyancy loss to the wake of thermal is not significant to the motion of the thermal, because the buoyant force within the wake is relatively small. For example, in the case as shown in Fig.3, the buoyancy loss to the wake is about 4% of the total buoyant force. This confirms that in the theoretical treatment for the conservative thermal the assumption that no buoyancy is lost to the wake of thermal seems to be valid[5]. The shape of the thermal changes gradually from a circle to an ellipse with the half width-to-length ratio H/L of about 0.62 at t=10s in both experiment and computation. We also found that the velocity fields of two symmetrical vortex structures are established soon after release. The velocity fields (Fig.3) reveals that the formation of wake is due to the velocity differences between the main part and the rear part of the thermal. Since velocity at the rear part is much smaller than the main part, the rear part is left behind as the main part moves forward. The maximum of velocity near the center of the thermal is about 3 times larger than mass center velocity V. During the early stages of the motion, the maximum of density excess appears near the center of cloud, and after some distance the phenomenon of double-peak distribution appears due to the entrainment of less dense fluid into the central part from the rear of thermal.

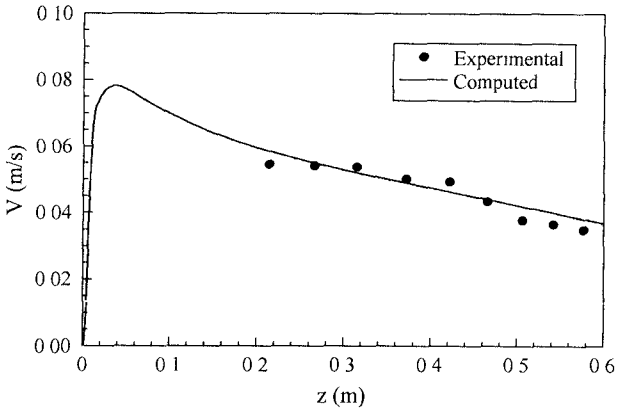

Fig.4 Mass center velocity V as a function of z

Fig.4 presents the mass center velocity V as a function of distance from the source z. This figure shows that the motion of the thermal has a fast acceleration and slow deceleration phase. The mass center velocity V reaches its maximum of 0.078 m/s at z=0.04m. Fig.4 also show that V is almost proportional to $z^{-1/2}$ during the deceleration stage.

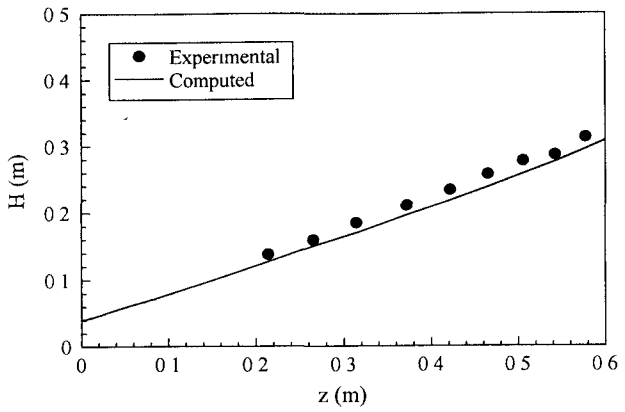

Fig.5 Half width H as a function of z

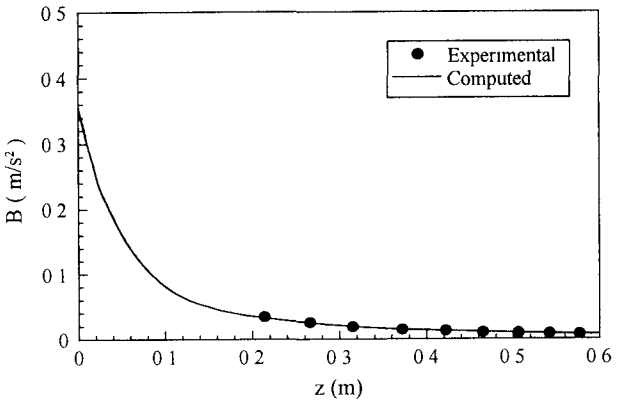

Fig.6 Average buoyant force B as a function of z

The symbols in the figure are average results of five runs under the same experimental conditions.

Experimental study by Akiyama et al.[5] found that half width of the thermal H increases linearly with distance z and the value of growth rate dH/dz is around 0.48. Baines and Hopfinger[4] also found the linear relationship between H and z in their studies on light thermals. Fig.5 shows that the computational results of H almost increase linearly with z and the values of H are close to the experimental data. The calculated value of dH/dz is found to be 0.45.

The average buoyant force B is defined as $B = g(\overline{\rho} - \rho_a)/\rho_a$, where $\overline{\rho}$ is the average density of the thermal. Fig.6 shows that B is almost proportional to z^{-2}. This is consistent with the theoretical result obtained by Akiyama et al.[5]

5. CONCLUSIONS

A large eddy simulation of 2-D heavy turbulent thermal has been performed. The eddy viscosity is evaluated by the Smagorinsky model and the governing equations are solved by the CCS scheme. The comparisons of computational results of main flow characteristics, including shape, size, mass center velocity and average buoyant force, with the experimental results show that the numerical simulation gives a good description of the thermal.

It is clearly demonstrated from the computation that the internal flow of the thermal is characterized by two symmetrical vortex structures and the density excess becomes a double-peak distribution after some distance. The computational results also show that the buoyancy loss to the wake occurs, but it does not affect significantly to the motion of the thermal.

ACKNOWLEDGEMENT: This study was supported by the Grant-in-Aid for Science Research (B) of the Ministry of Education and Culture, Japan, under the Grant No.08455232.

REFERENCES

1) Scorer, R.S.: Experiments on convection of isolated masses of buoyant fluid, *J. Fluid Mech.*, Vol.2, pp.583-594, 1957.
2) Wang, C.P.: Motion of a turbulent buoyant thermal in a calm stably stratified atmosphere, *The Physics of Fluids*, Vol.16, pp.744-749, No.6, 1973.
3) Escudier, M.P. and Maxworthy, T.: On the motion of turbulent thermals, *J. Fluid Mech.*, Vol.61, part 3, pp.541-552, 1973.
4) Baines, W.D. and Hopfinger, E.J.: Thermals with large density difference, *Atmospheric Environment*, Vol.18, No.6, pp.1051-1057, 1984.
5) Akiyama, J., Ura, M., Ying, X., Imamiya, M. and Suyama, M.: Flow characteristics of dense cloud instantaneously released into quiescent fluid, *Annual Journal of Hydraulic Engineering*, JSCE, Vol.42, pp.529-534, 1998 (in Japanese).
6) Nakatsuji, K., Tamai, M. and Murota, A., Dynamic behaviors of sand clouds in water, *Int Conf. Phys. Modelling of Transport and Dispersion*, M.I.T. Boston, 8C.1-8C.6, 1990.
7) Li, C.W.: Convection of particle thermals, *Journal of Hydraulic Research*, Vol.35, No.3, pp.363-376, 1997 .
8) Tamai, M. and Muraoka, K.: Numerical simulation on characteristics of turbidity transport generated in direct dumping of soil, *Annual Journal of Hydraulic Engineering*, JSCE, Vol.42, pp.541-546, 1998 (in Japanese).
9) Ahlberg, J.H., Nilson,E.N. and Walsh, J.L.: The theory of splines and their applications, Academic Press, New York, 1976.
10) Ying, X., Akiyama, J. and Ura, M.: The CCS method for two-dimensional advection and diffusion equation, *Proceeding of the West Japan Society of Civil Engineers*, pp.152-153, 1997.
11) Ying, X., Akiyama, J. and Ura, M.: Large eddy simulations of two-dimensional turbulent inclined plumes, *Annual Journal of Hydraulic Engineering*, JSCE, pp.1171-1176, 1998.

(Received September 30,1998)